

Title Page

**Subtype-Specific Sorting of The ET_A Endothelin Receptor by A
Novel Endocytic Recycling Signal for G Protein-Coupled Receptors**

Joachim D. Paasche, Toril Attramadal, Kurt Kristiansen, Morten P. Oksvold, Heidi K. Johansen,
Henrik S. Huitfeldt, Svein G. Dahl, and Håvard Attramadal

J.D.P., T.A., H.K.J., and H.A.

MSD Cardiovascular Research Center and Institute for Surgical Research,

Rikshospitalet University Hospital,

University of Oslo, Norway

M.P.O. and H.S.H.

Institute of Pathology,

Rikshospitalet University Hospital,

University of Oslo, Norway

K.K. and S.G.D.

Department of Pharmacology, Institute of Medical Biology,

University of Tromsø, Norway

Running Title Page

Running title: Endocytic Sorting Signal for ET_A receptor recycling

Corresponding author:

Håvard Attramadal, M.D., Ph.D.

Institute for Surgical Research, A3.1013

Rikshospitalet University Hospital

Sognsvannsveien 20

N-0027 Oslo, Norway

Phone: +47 23073520

E-mail: havard.attramadal@medisin.uio.no

Number of text pages: 39

Number of tables: 1

Number of figures: 9

Number of references: 43

Number of words in the Abstract: 249

Number of words in the Introduction: 690

Number of words in the Discussion: 1495

Abbreviations: DiI-LDL, dioctadecyl-tetramethylindocarbocyanine-low density lipoprotein; GFP, green fluorescent protein; GPCR, G protein-coupled receptor; GRK, G protein-coupled receptor kinase; PDZ, PSD-95/Dlg/ZO-1; Tf-Rhod, tetramethylrhodamine-labeled transferrin.

Abstract

We have previously reported that endocytic sorting of ET_A endothelin receptors to the recycling pathway is dependent on a signal residing in the cytoplasmic carboxyl-terminal region. The aim of the present work was to characterize the carboxyl-terminal recycling motif of the ET_A receptor. Assay of truncation mutants of the ET_A receptor with increasing deletions of the carboxyl-terminal tail revealed that amino acids 390 – 406 contained information critical for the ability of the receptor to recycle. This peptide sequence displayed significant sequence similarity to several protein segments confirmed by X-ray crystallography to adopt antiparallel β -strand structures (β -finger). One of these segments was the β -finger motif of nNOS (neuronal nitric oxide synthase) reported to function as an internal PDZ (PSD-95/Dlg/ZO-1) domain-binding ligand (PDZ ligand). Based on these findings, the three-dimensional structure of the recycling motif of ET_A receptor was predicted to attain a β -finger conformation acting as an internal PDZ ligand. Site-directed mutagenesis at residues that would be crucial to the structural integrity of the putative β -finger conformation or PDZ ligand function prevented recycling of the ET_A receptor. Analysis of more than 300 G protein-coupled receptors (GPCRs) identified 35 different human GPCRs with carboxyl-terminal sequence patterns that fulfilled the structural criteria of an internal PDZ ligand. Among these are several receptors reported to follow a recycling pathway. In conclusion, recycling of ET_A receptor is mediated by a motif with the structural characteristics of an internal PDZ ligand. This structural motif may represent a more general principle of endocytic sorting of GPCRs.

Introduction

The physiological effects of the vasoactive peptide endothelin-1 (ET-1)¹ are mediated by the ET_A and ET_B receptors, which belong to class A G protein-coupled receptors (GPCRs) (Yanagisawa, 1988). In the vasculature, ET_A receptors residing on smooth muscle cells mediate prolonged vasoconstriction, whereas ET_B receptors, which are located on the plasma membrane of endothelial cells, are primarily considered to cause NO-mediated vasodilatation (Yanagisawa, 1989). In addition, considerable evidence now also supports a role for the ET_B receptor in clearance of plasma ET-1 from the circulation (Berthiaume, 2000). We have previously shown that agonist-induced internalization of the two receptor subtypes depends on a mechanism involving G protein-coupled receptor kinase, arrestin, clathrin, and dynamin (Bremnes, 2000). After internalization, however, the two receptor subtypes are targeted to different intracellular fates. The ET_A receptor follows the recycling pathway through the pericentriolar recycling compartment and subsequently reappears on the plasma membrane, whereas the ET_B receptor is directed to lysosomes for degradation (Bremnes, 2000). In terms of physiological effects, rapid recycling of the ET_A receptor may provide basis for reestablishment of the signaling response, and thus, for the sustained vasoconstriction mediated by this receptor.

A key event of endocytic transport of signaling receptors is their sorting to either divergent recycling or degradative membrane pathways. The prevailing model proposes that internalized receptors are prevented from recycling by becoming sequestered and retained in multivesicular bodies (Sorkin, 2002). According to this model, recycling is considered the default destiny of membrane receptors not being targeted to lysosomes. The model is based mainly on studies of endocytic trafficking of the transferrin receptor and the epidermal growth factor

receptor (Mukherjee, 1997). Rapid recycling of these receptors has been reported even after all cytoplasmic residues have been removed (Mayor, 1993). This passive view of recycling has recently been challenged at least as far as GPCRs are concerned. Emerging evidence, including a previous report from our laboratory (Paasche, 2001), indicates that recycling of GPCRs is dependent on signals residing in the cytoplasmic carboxyl-terminal region (Cao, 1999; Hirakawa, 2003; Kishi, 2001; Tanowitz, 2003; Trejo, 1999). Analysis of carboxyl-terminally truncated ET receptors and ET_A/ET_B chimera revealed that lysosomal trafficking appears to be the "default" pathway without any requirement for cytoplasmic carboxyl-terminal sorting signals (Paasche, 2001). In contrast, recycling of the ET_A receptor was dependent on a signal residing in the carboxyl-terminal tail of this receptor subtype. So far, however, the structural characteristics of a motif involved in sorting of a GPCR to the recycling pathway has been determined for the β₂ adrenergic receptor (β₂-AR) only (Cao, 1999). The carboxyl-terminal end of the β₂-AR contains a structure or sequence pattern (DSSL) typically recognized by class I PDZ (PSD-95/Dlg/ZO-1) domain proteins (Hall, 1998). The PDZ ligand of the β₂-AR has been reported to bind EBP50/NHERF1 (Ezrin-radixin-moesin (ERM)-binding phosphoprotein-50/Na⁺/H⁺ exchange regulatory factor 1), and to promote recycling of the β₂-AR by linking the receptor to the actin cytoskeleton through the ERM-binding domain of EBP50 (Hall, 1998; Cao, 1999). Furthermore, when grafted onto the carboxyl-terminal end of the δ-opioid receptor (δ-OR), this four-residue sequence (DSL_L) was shown to re-route endocytosed δ-OR from the degradative to the recycling pathway (Gage, 2001). On the other hand, the carboxyl-terminal PDZ ligand of the β₁-AR does not appear to be critical for recycling of this receptor subtype (Xiang, 2003). Furthermore, many receptors that are efficiently sorted to the recycling pathway, including the ET_A receptor, lack classical carboxyl-terminal PDZ binding motifs (Bremnes, 2000; Hirakawa, 2003; Kishi, 2001;

Tanowitz, 2003; Trejo, 1999). Yet, for several of these receptors the cytoplasmic carboxyl-terminal region has been shown to provide signals critical for sorting of the receptors to the recycling pathway (Bremnes, 2000; Hirakawa, 2003; Kishi, 2001; Tanowitz, 2003; Trejo, 1999). Thus, the aim of the present study was to identify and characterize the structural motif in the carboxyl-terminal tail of the ET_A receptor that dictates recycling of the receptor. Bioinformatics and mutational analysis of ET_A receptor sorting provided several lines of evidence that an internal PDZ ligand of the carboxyl-terminal region targets the receptor to the recycling pathway. Furthermore, additional evidence suggests that internal PDZ ligands may represent a more general principle involved in sorting of many G protein-coupled receptors.

Materials and Methods

Plasmid Constructs

Subcloning of human transferrin receptor cDNA into pcDNA1 and of the open reading frame of human ET_A receptor into the mammalian expression vector pcDNA3 (pcDNA3-ET_A) has been described previously (Bremnes, 2000). The hemagglutinin (HA) epitope-tagged dominant negative EBP50 truncation mutant EBP50ΔERM in pcDNA3 was generously provided by Dr. Mark von Zastrow, University of California, San Francisco (Cao, 1999).

Construction of ET_A Receptor Truncation Mutants

Truncation mutants of the ET_A receptor with deletions of the cytoplasmic carboxyl-terminal tail were constructed in pcDNA3 by PCR directed mutagenesis. The truncation mutants ET_A-Δ417, ET_A-Δ406, ET_A-Δ401, ET_A-Δ398, ET_A-Δ394, and ET_A-Δ390 were made by replacement of D418, W407, G402, P399, M395, or S391, respectively, by stop codon and introduction of a *Xba*I restriction site downstream of the stop codon. The 3'-prime *Eco*RI-*Xba*I fragment of wild type ET_A (pcDNA3-ET_A) was replaced by the corresponding *Eco*RI/*Xba*I-digested PCR product to introduce the deletions indicated above. The cDNA constructs were verified by DNA sequence analysis using the dideoxy chain termination method. Construction of ET_A receptor with in-frame carboxyl-terminal fusion of green fluorescent protein (ET_A-GFP) in the mammalian expression vector pEGFP-N1 (BD Biosciences Clontech) has been described previously (Bremnes, 2000). ET_A-Δ406-GFP and ET_A-Δ401-GFP, i.e. ET_A receptor truncation mutants with in-frame fusion of GFP at the carboxyl-terminal truncation site were made by introduction of a *Bam*H1 restriction site at the terminal amino acid in pcDNA3-ET_A-Δ406 and pcDNA3-ET_A-Δ401 using PCR-

directed mutagenesis. The *EcoR1/BamH1* fragments of these modified vectors were subsequently transferred to *EcoR1/BamH1*-digested pEGFP-N1-ET_A-GFP to generate pEGFP-N1-ET_A-Δ406-GFP and pEGFP-N1-ET_A-Δ401-GFP, respectively.

Construction of ET_A Receptor Point Mutants

ET_A receptors with point mutations in the cytoplasmic carboxyl-terminal tail were constructed by site-directed circular mutagenesis using pcDNA3-ET_A as template and two complementary oligonucleotide primers harboring the desired mutation. The QuickChange site-directed mutagenesis kit (Stratagene) for circular mutagenesis was employed, and mutants were selected by *Dpn1* and verified by DNA sequence analysis using the dideoxy chain termination method.

Cell Lines and Transfection

CHO-K1 cells (ATCC no. CRL-61) were maintained, propagated, and transfected as previously described (Bremnes, 2000; Paasche, 2001). For fluorescence microscopy experiments, cells were plated onto glass coverslips before transfection. For cytosolic Ca²⁺ determination, CHO cells were grown within a 10 mm diameter polyethylene cylinder attached to the central part of a glass coverslip.

Kinetics of [¹²⁵I]-ET-1 Internalization and Recycling

Assay of internalization and externalization of wild type ET_A receptor and the ET_A receptor mutants were performed using receptor labeling with [¹²⁵I]-ET-1 (Amersham Biosciences) as described previously (Bremnes, 2000; Paasche, 2001). [¹²⁵I]-ET-1 binding to ET_A receptor is essentially irreversible and the sum of surface-bound and internalized [¹²⁵I]-ET-1 remained

constant during the assay. Thus, analysis of the fraction of receptors remaining intracellularly or on the surface of the plasma membrane as function of time enabled assay of receptor recycling as previously validated (Paasche, 2001).

Radioligand Binding

Radioligand binding analysis of membrane preparations of transiently transfected CHO cells was performed according to Elshourbagy et al. (Elshourbagy, 1993) with minor modifications (Bremnes, 2000).

Loading of CHO Cells with Fura-2 Acetoxymethyl Ester and Measurement of Cytosolic Ca²⁺ in Single Cells

Transiently transfected CHO cells on glass coverslips were washed once with Hank's balanced salt solution (HSS) and incubated in HSS solution containing 5 μ M Fura-2 and 0.025% Pluronic F127 for 30 min at 37 °C. After incubation, the cells were washed once and then incubated at 37 °C for 30 min before assay of cytosolic Ca²⁺ concentrations in response to stimulation with ET-1. The methodology and software for data acquisition and analysis of cytosolic Ca²⁺ concentrations in single cells have been described previously (Röttingen, 1995). In brief, the cells were illuminated at the excitation wavelengths 345 nm and 385 nm 2.5 times per second. Fluorescent images were collected by a CCD video camera, stored on a videotape and simultaneously digitized by a framegrabber controlled by a computer. Cytosolic Ca²⁺ concentrations were calculated from the ratio between fluorescence intensities at excitation wavelengths 345 nm and 385 nm at user-selected squares covering single cells. After recording of baseline fluorescence,

ET-1 was added (100 nM) and collection of fluorescent images were continued in order to measure agonist-stimulated Ca^{2+} levels.

Phosphoinositide Hydrolysis

ET-stimulated inositol phosphate generation was assayed in transfected CHO cells metabolically labeled with $3\mu\text{Ci}$ myo- $[\text{}^3\text{H}]$ inositol as described previously (Paasche, 2001).

Western Blot Analysis

To verify expression of the HA epitope-tagged carboxyl-terminal truncation mutant of EBP50, EBP50 Δ ERM (Cao, 1998), Western blot analysis of samples from untransfected and transiently transfected CHO cells was performed. The immunoblots were processed as described previously (Bremnes 2000), using anti-HA IgG $_{2a}$ and subsequently, horseradish peroxidase-conjugated anti-mouse IgG, and the ECL system (Amersham Biosciences) for detection of immunoreactivity.

Analysis of Intracellular Trafficking of Receptor-GFP Fusion Proteins by Confocal Laser Scan Microscopy

For analysis of ET receptor trafficking, transfected CHO cells attached to glass coverslips were placed on ice, washed, and preincubated with cycloheximide (10 mg/ml) in HSS for 30 minutes to prevent accumulation of newly synthesized ET $_A$ -GFP in the Golgi apparatus. The cells were subsequently incubated with ET-1 (100 nM) for 1 h at 4 °C in binding buffer (HSS containing 20 mM HEPES pH 7.4, 0.2% bovine serum albumin, 0.1% glucose and 10 mg/ml cycloheximide). Endocytosis of agonist-stimulated ET $_A$ -GFP or GFP-tagged ET $_A$ receptor mutants was initiated by rapidly changing the cell medium to 37 °C. The cells were incubated for various periods of

time at 37 °C in order to investigate the intracellular trafficking pathways of the different receptor mutants. The cells were subsequently fixed in 4% paraformaldehyde before mounting onto object slides using Mowiol (Hoechst). Cells were examined with Leica TCS SP confocal microscope equipped with an Ar (488 nm) and two He/Ne (543 and 633 nm) lasers. A Plan apochromat 100×/1.4 oil immersion objective was used. Multi-labeled images were acquired sequentially with a CCD camera. Images were processed and overlaid using Photoshop 7.0.

Uptake of Red Fluorescent Transferrin and LDL

Loading of the pericentriolar recycling compartment with 25 µg/ml tetramethylrhodamine-conjugated transferrin (Tf-Rhod; Molecular Probes) was performed in CHO cells cotransfected with ET receptor-GFP cDNA and cDNA for the human transferrin receptor as described previously (Bremnes, 2000). For labeling of lysosomes, LDL-DiI (Molecular Probes) was bound to the cells simultaneously with ET-1 at 4 °C. Internalization of the agonist-bound receptor was subsequently performed at 37 °C for 60 min allowing receptor-bound LDL to enter lysosomal compartments. The cells were fixed in 4% paraformaldehyde before mounting of the samples and investigation by confocal laser scan microscopy.

Structure Predictions of The Cytoplasmic Carboxyl-Terminal Region of The ET_A Receptor

The ICM Pro 3.0 program (Molsoft L.L.C., La Jolla, CA; available at www.molsoft.com) was utilized for modeling and computer graphics visualizations (Abagyan, 1994). Using a crystal structure of bovine rhodopsin as structural template (Palczewski, 2000), a three-dimensional model of the human ET_A receptor (Swiss-Prot # P25101) was constructed. In order to obtain evidence of a structural motif within the cytoplasmic carboxyl-terminal region of the ET_A

receptor, the PDB database of The Research Collaboratory for Structural Bioinformatics (www.rcsb.org) was searched for proteins with sequence similarity to the Q390 - N427 segment of the ET_A receptor. The National Center for Biotechnology Information (NCBI) BLAST software (Altschul, 1997) maintained by the Swiss Institute of Bioinformatics (<http://us.expasy.org/tools/blast/>) was employed to identify proteins in the PDB database with amino acid sequence similarities to the Q390 - N427 segment of the ET_A receptor. The structures of any identified proteins were retrieved and visualized computer graphically using the ICM software.

Probing The Cytoplasmic Carboxyl-Terminal Region of Mammalian GPCRs for Internal PDZ Interaction Motifs

Amino acid sequences for ~300 different mammalian family A GPCRs excluding the olfactory receptors, 15 different family B GPCRs and 22 different family C GPCRs were obtained from the Swiss Prot and TrEMBL protein sequence databases (Abagyan, 1994). The ClustalX 1.82 protein analysis program (CSC - Scientific Computing Ltd) was first used to obtain crude alignments of these sequences. The resulting alignments were further edited and analyzed with the BioEdit computer program. Thereafter, the carboxyl-terminal regions were retrieved from these alignments, starting from the positions corresponding to V372 of the human ET_A receptor (family A), E398 of the human secretin receptor (family B) and E865 of the human GABA_{B1} subunit (family C). The ICM 3.0 program was employed to search for putative internal PDZ ligand motifs in the carboxyl-terminal tail sequences using the following amino acid sequence pattern $\{[?]\}^5[ST][?][IVLMF]\{[?]\}^{3-6}[ST]\{[?]\}^4[RKH]\{[?]\}^3$. $\{[?]\}^n$ represents any n consecutive amino acids. [ST] represents either a serine or a threonine residue. The amino-terminal [ST] of

the sequence pattern corresponds to the P₋₂ position of the internal PDZ pseudopeptide. [IVLMF] represents a hydrophobic residue (P₀ position), i.e. isoleucine, valine, leucine, methionine, or phenylalanine. [RKH] represents any positively charged residue, i.e. arginine, lysine or histidine.

Results

Functional Characterization of Wild Type ET_A Receptor, ET_A Receptor Mutants and ET_A-GFP

Stimulation of CHO cells transfected with either wild type ET_A receptor or the truncation mutants ET_A-Δ406 or ET_A-Δ401 with ET-1 (100 nM) generated rapid elevations in intracellular calcium concentrations (Fig. 1A). Untransfected cells, however, did not respond to stimulation with ET-1. Peak calcium concentrations appeared to be slightly higher in cells transfected with the ET_A-Δ406 or ET_A-Δ401 truncation mutants than in ET_A wild type transfected cells, but these differences were not statistically significant. Thus, the ET_A receptor mutants were found to have similar capacities for generation of second messenger responses as their wild type counterpart. In frame carboxyl-terminal fusion of green fluorescent protein (GFP) was employed to investigate the intracellular trafficking pathways of ET_A receptor. As demonstrated in Fig. 1B, internalization of [¹²⁵I]-ET-1 in CHO cells transfected with ET_A-GFP showed that internalization of agonist-bound ET_A-GFP proceeded with similar kinetics as that of wild type ET_A receptor. Furthermore, the capacity of ET_A-GFP to mediate ET-1-stimulated inositol phosphate generation, as shown in Fig. 1C, was nearly identical to that of wild type ET_A receptor. Agonist-induced endocytosis of ET_A-GFP was also examined with confocal laser scan microscopy. CHO cells transfected with ET_A-GFP were incubated with ET-1 (100 nM) for 1h at 4 °C. Unbound ligand was subsequently removed and endocytosis of agonist-bound receptor was initiated by changing of the medium to 37 °C. As seen in Fig. 1D, ET_A-GFP is initially localized predominantly at the plasma membrane. However, within minutes after agonist-induced endocytosis of ET_A-GFP, the receptor was detected in a spot-like structure near the nucleus demonstrating agonist-dependent intracellular

transport. Fig. 1E demonstrates endocytosis and intracellular trafficking of Tf-Rhod in CHO cells transfected with human transferrin receptor. As shown, Tf-Rhod appears to be rapidly internalized and transported through endosomal vesicles to a perinuclear endosomal compartment. After 15 min Tf-Rhod is almost entirely located in the spot-like perinuclear structure previously demonstrated to represent the perinuclear recycling compartment (Presley, 1993). Accordingly, for optimal labeling of the recycling compartment in subsequent experiments, agonist-dependent endocytosis was allowed to proceed for 15 min.

Intracellular Trafficking of ET_A Receptor Mutants with Deletions of The Cytoplasmic Carboxyl-Terminal Tail

To identify the domain in the carboxyl-terminal tail of the ET_A receptor that mediates recycling, a series of deletion mutants were constructed by introducing stop codons at positions D418 (ET_A-Δ417), W407 (ET_A-Δ406), G402 (ET_A-Δ401), P399 (ET_A-Δ398), M395 (ET_A-Δ394), or S391 (ET_A-Δ390). The ligand binding characteristics of these truncated receptors did not differ significantly from that of wild type ET_A receptor (Table 1). As shown in Fig. 2, the ET_A-Δ406 truncation mutant showed a biphasic internalization curve similar to that of wild type ET_A receptor. The declining part of this curve pattern (representing increasing fractions of receptor reappearing at the surface of the plasma membrane) has previously been shown to reflect recycling of the ET_A receptor (Paasche, 2001). The ET_A-Δ417 mutant (not shown) also retained a biphasic internalization curve and hence the capability to undergo recycling. For the ET_A receptor mutants with truncations amino-terminal to Q406 (ET_A-Δ401, ET_A-Δ398, ET_A-Δ394, ET_A-Δ390), however, the time course of internalization shifted from a biphasic to a monophasic event as shown in Fig. 2. We have previously shown that the signal for recycling resides distal to amino

acid Q390 of ET_A (Paasche, 2001). Thus, the current observations provide evidence that the amino acid sequence 390 – 406 contains the critical information conferring the ability of the receptor to undergo recycling. To further investigate the intracellular trafficking pathways of the truncation mutants ET_A-Δ406 or ET_A-Δ401, green fluorescent protein (GFP) was fused to the carboxyl-terminal end of these receptor mutants for analysis of subcellular localization using fluorescence microscopy. ET_A-Δ406-GFP and ET_A-Δ401-GFP were transiently transfected into CHO cells and subjected to analysis of agonist-stimulated internalization. The GFP-tagged wild type ET_A receptor (ET_A-GFP) was analyzed in parallel for comparison. As shown in Fig. 3, after 15 min of ET-1 induced internalization, both ET_A-GFP and ET_A-Δ406-GFP accumulated in a perinuclear spot-like structure that was co-labeled with red fluorescent transferrin i.e. a prototypical marker of the perinuclear recycling compartment (Presley, 1993). ET-induced internalization of ET_A-Δ401-GFP, however, was associated with spread endosome-like vesicular structures throughout the cytoplasm with only minor colocalization in the recycling compartment. This finding indicates that the transport route of ET_A-Δ401 differs from that of ET_A-GFP and ET_A-Δ406-GFP. To investigate whether the spread vesicular distribution of internalized ET_A-Δ401 was consistent with transport to lysosomes, the lysosomal compartments of ET_A-Δ406-GFP- or ET_A-Δ401-GFP-transfected cells were labeled with red fluorescent LDL (DiI-LDL) (Handley, 1981). As shown in Fig. 4, neither ET_A-GFP nor ET_A-Δ406-GFP colocalized with red fluorescent LDL after 60 min of internalization. However, the spread endosome-like structures of internalized ET_A-Δ401-GFP demonstrated extensive colocalization with red fluorescent LDL (Fig. 4).

Identification and Characterization of A Motif in The Carboxyl-Terminal Tail of The ET_A Receptor that Dictates Receptor Recycling

Searching of the PDB database revealed that specific domains of rat CD2 (PDB # 1hng), human interferon- γ receptor α chain (IFN- γ R α) (PDB # 1fyh), and human neuronal nitrogen oxide synthase (nNOS) (PDB # 1qau) displayed significant similarities to the Q390-D411 peptide segment of ET_A (Fig. 5A). F103-Q124 of human nNOS, I131-T151 of human IFN- γ R α , and Y129-N149 residues of rat CD2 displayed 36%, 40%, and 40% amino acid similarities, respectively, to the Q390-D411 peptide segment of the human ET_A receptor. Furthermore, the identified segments of CD2, IFN- γ R α , and nNOS all contained anti-parallel β -strands adopting β -finger structures. Indeed, the β -finger of human nNOS has been reported to function as an internal PDZ-ligand (Christopherson, 1999). In this motif, the proximal β -strand (also referred to as the pseudopeptide motif) structurally mimics distal carboxyl-terminal PDZ-ligands in its sequence-specific interaction with one of the PDZ domains of syntrophin. Analysis of the crystal structure of the PDZ-ligand of human nNOS in complex with the PDZ domain of syntrophin, revealed that the hydrophobic phenylalanine at the end of the proximal β -strand (G-strand) is exposed by a sharp β -turn and mimics the free carboxylate group normally required for the hydrophobic P₀ position of a carboxyl-terminal ligand (Harris, 2001). Based on sequence similarities between the ET_A receptor and the proteins shown in Fig. 5A and B, and using the structure of nNOS as a template, a three-dimensional model of the K392-H410 peptide sequence of the ET_A receptor was built. In the predicted structure, as shown in Fig. 5C, the proximal β -strand was found to contain a sequence conforming to Class 1 PDZ ligands with V398 and T396 of ET_A representing the P₀ and the P₋₂ positions, respectively, of the putative PDZ ligand.

Intracellular Trafficking of ET_A Receptors with Mutations that Perturb The PDZ

Recognition Sequence or Structural Integrity of The β -Finger

To provide further evidence that the 390-406 peptide sequence of ET_A possesses PDZ ligand properties, we used site-directed mutagenesis at residues that would be crucial to the structural integrity of the putative ligand. Fig. 6A and B show the kinetics of agonist-induced internalization of ET_A wild type and ET_A receptor mutants with substitutions perturbing the proximal strand of the β -finger, i.e. the strand containing the ligand directly interacting with a PDZ domain-containing protein. Agonist-stimulated internalization of the ET_A T396A/S397A mutant was substantially impaired as compared to its wild type counterpart (Fig. 6A). Furthermore, the internalization curve was shifted from a biphasic to a monophasic event, which indicates that mutations of the P₋₁ and P₋₂ positions of the putative PDZ ligand prevent recycling. Mutations of V398 which represents the hydrophobic P₀ position into alanine or glycine (Fig. 6B) did not affect the initial rate of internalization, but abolished the biphasic curve pattern indicating severely perturbed recycling. In order to test our structural model further, mutations at residues that would perturb the distal strand of the β -finger were also made. As shown in Fig. 6C and D, agonist-induced internalization of the ET_A-T403A/S404A mutant exhibited a monophasic internalization curve similar to that of the ET_A-T396A/S397A mutant where both the initial rate of internalization and recycling capabilities were affected. The I405A and I405G mutations had less dramatic, albeit similar effects as V398A and V398G mutations. Inhibition of recycling was more pronounced upon mutation to alanine but was observed for both the ET_A-I405A and ET_A-I405G mutants (Fig. 6D). To study the intracellular trafficking pathways of these point-mutated receptors, GFP fusion proteins of ET_A-T396A/S397A and ET_A-T403A/S404A mutants were made. Agonist-stimulated internalization of receptor was investigated together with simultaneous

uptake of red fluorescent Tf-Rhod or DiI-LDL as described under *Materials and Methods*. As shown in Fig. 3, neither the ET_A-T396A/S397A-GFP nor ET_A-T403A/S404A-GFP mutants colocalized with transferrin receptor in the pericentriolar recycling compartment as opposed to ET_A-GFP. However, in cells transfected with ET_A-T396A/S397A-GFP or ET_A-T403A/S404A-GFP, labeled with DiI-LDL, and stimulated with ET-1 for 60 min extensive colocalization of receptor and DiI-LDL was detected in lysosomes (Fig. 4). Taken together, these results support our hypothesis that recycling of ET_A receptor is mediated via PDZ domain interactions.

Analysis of T396, S397, T403 and S404 of ET_A as Potential Sites of Phosphorylation

As described above, substitutions of serine and threonine in the ET_A-T396A/S397S or ET_A-T403A/S404A double mutants affected not only the recycling capabilities but also the rate of internalization. Based on these observations we examined whether the indicated threonine and serine residues were sites of phosphorylation by introducing negative charge in the form of an aspartate residue that could mimic a phosphorylated state in these positions. We constructed mutants of ET_A-Δ406 and “full length” ET_A receptors where T396, S397, T403 and S404 were substituted with aspartate. Mutations into alanine were also made for parallel comparison. As shown in Fig. 7A and B, the aspartate and alanine substitutions of “full length” ET_A and ET_A-Δ406 abolished the biphasic internalization kinetics and significantly reduced the rate of internalization in a near identical manner. From these observations we conclude that receptor internalization and recycling are similarly affected upon mutation to alanine or aspartate.

Effect of A Dominant Negative EBP50 Mutant on Agonist-Stimulated Internalization and Recycling of The ET_A Receptor

To investigate whether or not recycling of the ET_A receptor is dependent on EBP50, we used a dominant negative truncation mutant of EBP50 (EBP50ΔERM) that lacks the ERM-binding domain but retains the PDZ domain reported to be required for interaction with the β₂-AR (Hall, 1998). CHO cells were transfected with the ET_A receptor alone or together with EBP50ΔERM. Western blot analysis, as shown in Fig. 8, confirmed the expression of EBP50ΔERM in the transiently transfected cells. The biphasic internalization kinetics of the ET_A receptor, which indicates recycling, was not altered upon expression of EBP50ΔERM (Fig. 8).

Probing for Internal PDZ Ligand Motifs in GPCRs

A specific sequence pattern required to fulfill the structural criteria of an internal PDZ ligand (described under *Materials and Methods*) were defined and used to construct an algorithm that could be employed to screen GPCRs. Analysis of the carboxyl-terminal regions of more than 300 mammalian family A, B and C GPCRs, starting after predicted endpoints of transmembrane helix 7, revealed 35 different human GPCRs that fulfilled the sequence criteria of internal PDZ ligand motif. Fig. 9 shows alignment of the identified carboxyl-terminal sequences of 27 human GPCRs identified in the above analysis for which the cognate ligand is known and 8 orphan GPCRs.

Discussion

In the present study, the carboxyl-terminal motif of ET_A receptor that dictates receptor recycling has been identified and characterized. Structural modeling and mutagenesis of the cytoplasmic carboxyl-terminal region of ET_A receptor revealed that receptor recycling is mediated by a motif with the structural characteristics of an internal PDZ ligand.

Composite data from studies of ET_A and ET_B receptor chimera where the carboxyl-terminal tail of the receptors were interchanged (Paasche, 2001), and from studies of increasing truncations of the carboxyl-terminal region of ET_A, revealed that the 17 amino acid polypeptide segment Q390-Q406 of ET_A receptor constitutes the minimal peptide sequence required to provide a functional signal for recycling. Surprisingly, the identified polypeptide segment was part of a slightly larger segment (Q390-D411) of the carboxyl-terminal region of ET_A that displayed striking similarities to peptide sequences of nNOS, IFN- γ R α and CD2 for which a common secondary and tertiary structure had been determined. The shared structure of the latter proteins consisted of anti-parallel β -strands forming β -fingers that in nNOS have been reported to function as a PDZ ligand (Hillier, 1999). Although the crystal structure of the ET_A receptor has not yet been determined, prediction of the secondary and tertiary structures of the Q390-D411 polypeptide segment of ET_A receptor revealed that this segment may also consist of anti-parallel β -strands attaining β -finger conformation. The proximal and distal β -strands of the putative β -finger could be supported by several hydrogen bonds between residues within the Q390-D411 polypeptide segment, one of which was a hydrogen bond typically found between the first and the fourth residue of the loop between the β -strands. The latter is considered crucial in stabilizing the β -turn (Coligan, 2004). Additional lines of evidence also reported in this study consistently supported involvement of the putative β -finger of ET_A in receptor recycling. Targeted mutations

of residues within the proximal β -strand (ET_A-T396A/S397A, ET_A-V398A, ET_A-V398G, ET_A-T403A/S404A, ET_A-I405A, ET_A-I405G), or distal β -strand (ET_A-T403A/S404A, ET_A-I405A, ET_A-I405G) all disrupted recycling of ET_A receptor. These observations indicate that mutations that affect the structural integrity of the β -finger abolish receptor recycling. However, in order to provide unequivocal evidence of a PDZ-mediated mechanism of ET_A receptor recycling, binding of the putative β -finger and a PDZ-containing protein would have to be demonstrated and implicated a role in receptor recycling. Strikingly, the proximal β -strand of the putative β -finger of ET_A also contained a pseudopeptide sequence conforming to the canonical class I PDZ ligand similar to that of the proximal β -strand of the nNOS β -finger. According to the predicted β -finger of ET_A, V398 represents the indispensable hydrophobic residue at the P₀ position of the putative PDZ ligand. As demonstrated in the present study, alanine substitution of the P₋₂, P₋₁, or P₀ residues of the PDZ pseudopeptide ligand in the proximal β -strand essentially eliminated recycling of ET_A receptor. These results correlate with the loss of function caused by alanine substitution of the corresponding PDZ pseudopeptide residues (T109A or F111A at the P₋₂ and P₀ positions, respectively) of nNOS (Harris, 2001).

Comparing the putative β -finger of ET_A receptor with that of nNOS also revealed conservation of a positive residue in the distal β -strand. R121 in the distal β -strand of nNOS forms a salt bridge with D62 and plays important role in binding of nNOS to the PDZ domain of syntrophin, presumably by stabilizing the β -finger formation (Harris, 2001). The specific function of K408 in the putative β -finger motif of ET_A receptor, i.e. the positive residue aligning with R121 of the distal β -strand nNOS, is unclear since this residue is removed in the ET_A- Δ 406 truncation mutant which is still capable of recycling. However, it has been reported that the β -

finger of nNOS is a fairly rigid structure, which even by itself, separate from nNOS, may retain some residual hairpin structure (Wang, 2000).

Previous reports have shown that agonist-stimulated desensitization and internalization of ET_A and ET_B receptors depend on GRK-catalyzed phosphorylation of serine and threonine residues in the cytoplasmic carboxyl-terminal region (Bremnes, 2000; Freedman, 1997). However, the specific residues of agonist-occupied ET_A receptors phosphorylated by GRK have yet to be determined. Conceivably, introduction of negative charge by phosphorylation of any serine or threonine residue of the carboxyl-terminal region may to some extent relieve intramolecular constraints sufficient to promote binding of β -arrestin with subsequent desensitization and internalization of the receptor. However, mimicking of ET_A receptor phosphorylation by substituting the indicated threonine and serine residues with aspartic acid (ET_A-T396D/S397D; ET_A-T403D/S404D) did not lead to increased rates of agonist-induced internalization. Rather, the aspartic acid substitutions impaired agonist-induced internalization to similar extent as alanine substitution of the same residues. (ET_A-T396A/S397A; ET_A-T403A/S404A). Thus, the reduced initial rates of agonist-induced internalization of the ET_A receptor mutants do not appear to be due to loss of GRK-catalyzed phosphorylation. A more plausible interpretation of the observed findings is that substitution of the serine and threonine residues of the proximal and distal β -strands disrupt the β -finger and thereby abolish ET_A receptor recycling. As serially connected mechanisms, impaired endosomal trafficking may also impact on the initial step of endocytosis, i.e. agonist-induced internalization of the ET_A receptor.

To our knowledge, this is the first demonstration implicating a putative internal PDZ ligand structure in endocytic sorting of a GPCR. An imminent issue then, was to what extent the putative internal PDZ ligand of ET_A receptor might represent a more widely employed principal

in endocytic sorting of GPCRs. Interestingly, as many as 35 different GPCRs fulfilled the principal criteria of an internal PDZ ligand motif. However, our search parameters only entailed class I PDZ domains. In this respect, inclusion of parameters covering class II and III PDZ domain proteins could potentially identify even more GPCR with internal PDZ ligand motifs. As shown in Fig. 9, the loop connecting the antiparallel β -strands of the putative β -finger structures of the aligned GPCRs consists of varying number of residues. Indeed, the variation in loop length allowed in the search parameters for β -finger-like PDZ ligand motifs in GPCRs was supported by evidence of maintained PDZ binding affinity upon insertion of additional residues in the β -turn region of the PDZ ligand of nNOS (Harris, 2001).

Among the human GPCRs shown in Fig. 9 are several receptors that have been reported to follow intracellular recycling pathways, i.e. the α_{1D} -adrenergic, AT₁ angiotensin, NK₁ neurokinin, Y₁ neuropeptide, LH luteinizing hormone, 5-HT_{2A} serotonin, SST₃ somatostatin, and V_{1A} vasopressin receptors (Kishi, 2001; Benya, 1994; Bhattacharyya, 2002; Chauvin, 2002; Garland, 1996; Gicquiaux, 2002; Hein, 1997; Innamorati, 1999; Kreuzer, 2001; McCune, 2000; Tseng, 1995; Marchese, 2001). Conversely, peptide sequences with similarity to the search parameters could not be identified in GPCRs sorting to lysosomes, e.g. the ET_B receptor, PAR-1, CXCR4 chemokine receptor, δ -opioid receptor and rat LH receptor (Bremnes, 2000; Kishi, 2001; Trejo, 1999; Gage, 2001; Marchese, 2001). Thus, the proposed model of internal PDZ ligand recognition appears to be a consistent mechanism for sorting GPCRs to the recycling pathway. The rat and human LH receptor homologs deserve special attention because of divergent sorting to lysosomes and endocytic recycling, respectively (Kishi, 2001). Interestingly, the primary structure of rat LH receptor differs from its human receptor homolog at residues critical to maintain the putative PDZ ligand-containing β -finger. Thus, rat LH receptor may be regarded as

a naturally occurring variant of human LH receptor that does not contain an operative PDZ ligand. This contention is supported by several reports of point mutations or deletion of amino acids in the carboxyl-terminal region of human LH receptor that divert the receptor from the recycling pathway to the lysosomal trafficking pathway (Kishi, 2001; Galet, 2004; Hirakawa, 2003). Indeed, these targeted amino acids were apparently all critical to maintain the PDZ pseudopeptide ligand or β -finger conformation according to our proposed model. Recently, a report by Ascoli and colleagues demonstrated that efficient recycling was also shown to be dependent on the upstream hydrophobic amino acid L683. According to the alignment in Fig. 9, L683 may represent the "0-position" of a putative PDZ ligand-containing β -finger formation.

Although sorting of GPCRs to the recycling pathway may depend on uniform mechanisms, different PDZ domain proteins may be involved. For example involvement of EBP50 does not appear to be a consistent finding (Cao, 1999; Kishi, 2001). In the present study a dominant negative deletion mutant of EBP50 (EBP50 Δ), lacking the ERM binding domain, did not affect recycling of the ET_A receptor despite massive expression of EBP50 Δ .

In the present study, bioinformatic and mutational analysis provide strong evidence that recycling of the ET_A receptor is mediated by a motif with the structural characteristics of an internal PDZ ligand. This motif which is lacking in the carboxyl-terminal region of ET_B endothelin receptors, provides a mechanism of the divergent sorting of the ET_A and ET_B receptor subtypes. Furthermore, we provide evidence that internal PDZ ligand motifs may represent a more general principle of endocytic sorting of GPCRs. The important challenge of the future will be to identify the protein that recognizes and binds the putative PDZ ligand motif of ET_A receptor and directs the receptor to the recycling pathway.

References

Abagyan R and Totrov M (1994) Biased probability Monte Carlo conformational searches and electrostatic calculations for peptides and proteins. *J Mol Biol* **235**:983-1002.

Altschul SF, Madden TL, Schaffer AA, Zhang J, Zhang Z, Miller W, and Lipman DJ (1997) Gapped BLAST and PSI-BLAST: a new generation of protein database search programs. *Nucleic Acids Res* **25**:3389-3402.

Benya RV, Kusui T, Shikado F, Battey JF, and Jensen RT (1994) Desensitization of neuromedin B receptors (NMB-R) on native and NMB-R-transfected cells involves down-regulation and internalization. *J Biol Chem* **269**:11721-11728.

Berthiaume N, Yanagisawa M, Labonte J, and D'Orleans-Juste P (2000) Heterozygous Knock-Out of ET_B Receptors Induces BQ-123-Sensitive Hypertension in the Mouse. *Hypertension*. **36**:1002-1007.

Bhattacharyya S, Puri S, Miledi R, and Panicker MM (2002) Internalization and recycling of 5-HT_{2A} receptors activated by serotonin and protein kinase C-mediated mechanisms. *Proc Natl Acad Sci USA* **99**:14470-14475.

Bremnes T, Paasche JD, Mehlum A, Sandberg C, Bremnes B, and Attramadal H (2000) Regulation and intracellular trafficking pathways of the endothelin receptors. *J Biol Chem* **275**:17596-17604.

Cao TT, Deacon HW, Reczek D, Bretscher A, and von Zastrow M (1999) A kinase-regulated PDZ-domain interaction controls endocytic sorting of the β_2 -adrenergic receptor. *Nature* **401**:286-290.

Cao TT, Mays RW, and von Zastrow M (1998) Regulated endocytosis of G-protein-coupled receptors by a biochemically and functionally distinct subpopulation of clathrin-coated pits. *J Biol Chem* **273**:24592-24602.

Chauvin S, Bencsik M, Bambino T, and Nissenson RA (2002) Parathyroid hormone receptor recycling: role of receptor dephosphorylation and β -arrestin. *Mol Endocrinol* **16**:2720-2732.

Christopherson KS, Hillier BJ, Lim WA, and Brecht DS (1999) PSD-95 assembles a ternary complex with the N-methyl-D-aspartic acid receptor and a bivalent neuronal NO synthase PDZ domain. *J Biol Chem* **274**:27467-27473.

Coligan ZE, Dunn BM, Speicher DW, and Wingfield PT Current Protocols in Protein Science. 17.1.1-17.1.189. 2004. John Wiley and Sons, Inc.

Elshourbagy NA, Korman DR, Wu HL, Sylvester DR, Lee JA, Nuthalaganti P, Bergsma DJ, Kumar CS, and Nambi P (1993) Molecular characterization and regulation of the human endothelin receptors. *J Biol Chem* **268**:3873-3879.

Freedman NJ, Ament AS, Oppermann M, Stoffel RH, Exum ST, and Lefkowitz RJ (1997) Phosphorylation and desensitization of human endothelin A and B receptors - Evidence for G protein-coupled receptor kinase specificity. *J Biol Chem* **272**:17734-17743.

Gage RM, Kim KA, Cao TT, and von Zastrow M (2001) A transplantable sorting signal that is sufficient to mediate rapid recycling of G protein-coupled receptors. *J Biol Chem* **276**:44712-44720.

Galet C, Hirakawa T, and Ascoli M (2004) The postendocytotic trafficking of the human lutropin receptor is mediated by a transferable motif consisting of the C-terminal cysteine and an upstream leucine. *Mol Endocrinol* **18**:434-446.

Garland AM, Grady EF, Lovett M, Vigna SR, Frucht MM, Krause JE, and Bunnett NW (1996) Mechanisms of desensitization and resensitization of G protein-coupled neurokinin1 and neurokinin2 receptors. *Mol Pharmacol* **49**:438-446.

Gicquiaux H, Lecat S, Gaire M, Dieterlen A, Mely Y, Takeda K, Bucher B, and Galzi JL (2002)

Rapid internalization and recycling of the human neuropeptide Y Y₁ receptor. *J Biol Chem*

277:6645-6655.

Hall RA, Premont RT, Chow CW, Blitzer JT, Pitcher JA, Claing A, Stoffel RH, Barak LS,

Shenolikar S, Weinman EJ, Grinstein S, and Lefkowitz RJ (1998) The β_2 -adrenergic receptor interacts with the Na⁺/H⁺-exchanger regulatory factor to control Na⁺/H⁺ exchange. *Nature*

392:626-30.

Handley DA, Arbeeny CM, Witte LD, and Chien S (1981) Colloidal gold - low density

lipoprotein conjugates as membrane receptor probes. *Proc Natl Acad Sci USA* **78**:368-377.

Harris BZ, Hillier BJ, and Lim WA (2001) Energetic determinants of internal motif recognition by PDZ domains. *Biochemistry* **40**:5921-5930.

Hein L, Meinel L, Pratt RE, Dzau VJ, and Kobilka BK (1997) Intracellular trafficking of

angiotensin II and its AT₁ and AT₂ receptors: Evidence for selective sorting of receptor and

ligand. *Mol Endocrinol* **11**:1266-1277.

Hillier BJ, Christopherson KS, Prehoda KE, Brecht DS, and Lim WA (1999) Unexpected modes of PDZ domain scaffolding revealed by structure of nNOS-syntrophin complex. *Science* **284**:812-815.

Hirakawa T, Galet C, Kishi M, and Ascoli M (2003) GIPC binds to the human lutropin receptor (hLHR) through an unusual PDZ domain binding motif, and it regulates the sorting of the internalized human choriogonadotropin and the density of cell surface hLHR. *J Biol Chem* **278**:49348-49357.

Innamorati G, Sadeghi H, and Birnbaumer M (1999) Phosphorylation and recycling kinetics of G protein-coupled receptors. *J Recept Signal Transduct Res* **19**:315-326.

Kishi M, Liu X, Hirakawa T, Reczek D, Bretscher A, and Ascoli M (2001) Identification of two distinct structural motifs that, when added to the C-terminal tail of the rat LH receptor, redirect the internalized hormone-receptor complex from a degradation to a recycling pathway. *Mol Endocrinol* **15**:1624-1635.

Kreuzer OJ, Krisch B, Dery O, Bunnett NW, and Meyerhof W (2001) Agonist-mediated endocytosis of rat somatostatin receptor subtype 3 involves β -arrestin and clathrin coated vesicles. *J Neuroendocrinol* **13**:279-287.

Marchese A and Benovic JL (2001) Agonist-promoted ubiquitination of the G protein-coupled receptor CXCR4 mediates lysosomal sorting. *J Biol Chem* **276**:45509-45512.

Mayor S, Presley JF, and Maxfield FR (1993) Sorting of membrane components from endosomes and subsequent recycling to the cell surface occurs by a bulk flow process. *J Cell Biol* **121**:1257-1269.

McCune DF, Edelmann SE, Olges JR, Post GR, Waldrop BA, Waugh DJ, Perez DM, and Piascik MT (2000) Regulation of the cellular localization and signaling properties of the α_{1B} - and α_{1D} -adrenoceptors by agonists and inverse agonists. *Mol Pharmacol* **57**:659-666.

Mukherjee S, Ghosh RN, and Maxfield FR (1997) Endocytosis. *Physiol Rev* **77**:759-803.

Opgenorth TJ, Wessale JL, Dixon DB, Adler AL, Calzadilla SV, Padley RJ, and Wu-Wong JR (2000) Effects of endothelin receptor antagonists on the plasma immunoreactive endothelin-1 level. *J Cardiovasc Pharmacol* **36**:Suppl-6.

Paasche JD, Attramadal T, Sandberg C, Johansen HK, and Attramadal H (2001) Mechanisms of endothelin receptor subtype-specific targeting to distinct intracellular trafficking pathways. *J Biol Chem* **276**:34041-34050.

Palczewski K, Kumasaka T, Hori T, Behnke CA, Motoshima H, Fox BA, Le TI, Teller DC, Okada T, Stenkamp RE, Yamamoto M, and Miyano M (2000) Crystal structure of rhodopsin: A G protein-coupled receptor. *Science* **289**:739-745.

Presley JF, Mayor S, Dunn KW, Johnson LS, McGraw TE, and Maxfield FR (1993) The End2 mutation in CHO cells slows the exit of transferrin receptors from the recycling compartment but bulk membrane recycling is unaffected. *J Cell Biol* **122**:1231-1241.

Røttingen JA, Enden T, Camerer E, Iversen JG, and Prydz H (1995) Binding of human factor VIIa to tissue factor induces cytosolic Ca²⁺ signals in J82 cells, transfected COS-1 cells, Madin-Darby canine kidney cells and in human endothelial cells induced to synthesize tissue factor. *J Biol Chem* **270**:4650-4660.

Sorkin A and von Zastrow M (2002) Signal transduction and endocytosis: Close encounters of many kinds. *Nat Rev Mol Cell Biol* **3**:600-614.

Tanowitz M and von Zastrow M (2003) A novel endocytic recycling signal that distinguishes the membrane trafficking of naturally occurring opioid receptors. *J Biol Chem* **278**:45978-45986.

Trejo J and Coughlin SR (1999) The cytoplasmic tails of protease-activated receptor-1 and substance P receptor specify sorting to lysosomes versus recycling. *J Biol Chem* **274**:2216-2224.

Tseng MJ, Detjen K, Struk V, and Logsdon CD (1995) Carboxyl-terminal domains determine internalization and recycling characteristics of bombesin receptor chimeras. *J Biol Chem* **270**:18858-18864.

Wang P, Zhang Q, Tochio H, Fan JS, and Zhang M (2000) Formation of a native-like beta-hairpin finger structure of a peptide from the extended PDZ domain of neuronal nitric oxide synthase in aqueous solution. *Eur J Biochem* **267**:3116-3122.

Xiang Y and Kobilka B (2003) The PDZ-binding motif of the β_2 -adrenoceptor is essential for physiologic signaling and trafficking in cardiac myocytes. *Proc Natl Acad Sci USA* **100**:10776-10781.

Yanagisawa M, Kurihara H, Kimura S, Tomobe Y, Kobayashi M, Mitsui Y, Yazaki Y, Goto K, and Masaki T (1988) A novel potent vasoconstrictor peptide produced by vascular endothelial cells. *Nature* **332**:411-415.

Yanagisawa M and Masaki T (1989) Endothelin, a novel endothelium-derived peptide. Pharmacological activities, regulation and possible roles in cardiovascular control. *Biochem Pharmacol* **38**:1877-1883.

Footnotes

This work was supported by the MSD Cardiovascular Research Fund and grants from the National Research Council and the Norwegian Council on Cardiovascular Disease.

Legends for Figures

Fig. 1 Functional characteristics of wild type ET_A receptor, carboxyl-terminally truncated ET_A receptors and ET_A-GFP fusion protein. (A) Time course of cytosolic Ca²⁺ concentrations in ET-1 stimulated CHO cells transiently transfected with wild type ET_A (····) receptor or the ET_A truncation mutants ET_A-Δ406 (—) and ET_A-Δ401 (---). The cells were loaded with Fura-2 as described under *Materials and Methods*. ET-1 (100 nM) was added 30 seconds after recording of light emission was initiated (arrow). Untransfected cells (—) stimulated with ET-1 were used as control of background levels. The data are mean of at least 80 cells from three independent experiments. (B) Internalization kinetics of [¹²⁵I]-ET-1 in CHO cells transiently transfected with wild type ET_A receptor or ET_A receptor with carboxyl-terminal fusion of GFP. Data are mean ± S.D. of three parallel wells and representative of at least three independent experiments. (C) Inositol phosphate accumulation in CHO cells transiently transfected with wild type ET_A receptor or ET_A-GFP stimulated in the absence or presence of ET-1 (100 nM). Data are mean ± S.D. of three parallel wells and representative of at least three independent experiments. (D) Photomicrographs demonstrating ET-1-induced endocytosis of ET_A-GFP in CHO cells. CHO cells on cover glass were transiently transfected with ET_A-GFP and analysed by confocal laser scan microscopy at 0, 15 and 60 min after initiation of ET-1 induced internalization. Cells were pretreated with 10 mg/ml cycloheximide for 30 min before addition of ET-1 (100 nM) and during the entire uptake period to clear newly synthesized receptor-GFP fusion protein from Golgi. The cells were subsequently fixed in paraformaldehyde at 4 °C and investigated by confocal laser scan microscopy. (E) Internalization of Tf-Rhod in CHO cells transfected with human transferrin

receptor. The cells were fixed in paraformaldehyde at the indicated time points after addition of Tf-Rhod and analyzed by confocal laser scan microscopy. Note that Tf-Rhod becomes highly enriched in a perinuclear compartment after 15 minutes of internalization.

Fig. 2 Intracellular trafficking of ET_A receptor with increasing truncation of the carboxyl-terminal region. Internalization kinetics of [¹²⁵I]-ET-1 in CHO cells transiently transfected with wild type ET_A (●) or the ET_A receptor truncation mutants ET_A-Δ406 (∇), ET_A-Δ401 (▼) and ET_A-Δ390 (○). 24 hours after transfection CHO cells were incubated with [¹²⁵I]-ET-1 (25 pM in 1 ml) for 3 h at 4 °C to label surface ET_A receptors. The internalization assay was initiated by rapid transfer of the cells to 37 °C for the time indicated. The fraction of intracellular receptor at each time point was measured as described under *Materials and Methods*. Inlet: Agonist-bound receptor (fmol/well) at plasma membrane surface at t = 0. Data are mean ± S.D. of three parallel wells and representative of at least three independent experiments.

Fig. 3 Subcellular localization of agonist-stimulated GFP-tagged ET_A wild type receptor and ET_A receptor with mutations affecting the putative carboxyl-terminal β-finger and internal PDZ ligand. Probing for receptor colocalization with transferrin in the recycling compartment. Photomicrographs of confocal laser scan microscopic analysis of CHO cells cotransfected with ET_A-GFP, ET_A-Δ406-GFP, ET_A-Δ401-GFP, ET_A-T396A/S397A-GFP, or ET_A-T403A/S404A-GFP and transferrin receptor. After binding of ET-1 (0.1 μM) at 4 °C, agonist-stimulated internalization of the ET receptors was analyzed after 15 min at 37 °C. Tf-Rhod was added during the 15 min period for simultaneous labeling of the perinuclear recycling

compartment. As shown in the overlays to the right, ET_A-GFP and ET_A-Δ406-GFP display prominent colocalization with transferrin receptor. ET_A-Δ401-GFP, ET_A-T396A/S397A-GFP or ET_A-T403A/S404A-GFP on the other hand, exhibit spread vesicular distribution lacking colocalization with transferrin receptor. Bar is 10 μM.

Fig. 4. Subcellular localization of agonist-stimulated GFP-tagged ET_A wild type receptor and ET_A receptor with mutations affecting the putative carboxyl-terminal β-finger and internal PDZ ligand. Probing for receptor colocalization with LDL in lysosomes.

Photomicrographs of confocal laser-scan microscopic analysis of CHO cells transiently transfected with ET_A-GFP, ET_A-Δ406-GFP, ET_A-Δ401-GFP, ET_A-T396A/S397A-GFP, or ET_A-T403A/S404A-GFP. Agonist-induced receptor internalization was performed for 60 min together with DiI-LDL to probe for lysosomal sorting. As shown in the overlays to the right, the spread vesicular distribution of ET_A-Δ401-GFP, ET_A-T396A/S397A-GFP and ET_A-T403A/S404A-GFP cococalized with LDL in lysosomes. ET_A-GFP and ET_A-Δ406-GFP could not be detected in DiI-LDL-labeled lysosomes. Bar is 10 μM.

Fig. 5 Analysis of the primary and secondary structures of the Q390-D411 peptide sequence of the ET_A receptor. The Q390-D411 sequence of the ET_A receptor aligned with rat CD2 (A), human INF-γRα (A), and human nNOS (B). The secondary structures of the aligning sequences of CD2, INF-γRα and nNOS as determined by X-ray crystallographic studies are indicated with arrows (β-strand structure) and lines (coil structure). The indicated sequence of nNOS is reported

to form a β -finger motif operating as an internal PDZ ligand. C. Predicted structure of the K392-H410 peptide sequence of the ET_A receptor. The predicted sequence consists of two antiparallel β -strands forming a β -finger. The proximal β -strand contains the sequence pattern recognized by class 1 PDZ domains, where the V398 represents the “P₀ position” of the pseudopeptide ligand.

Fig. 6 Intracellular trafficking of ET_A receptors with mutations at selected residues that would perturb the β -finger or internal PDZ ligand function. A-D. Internalization kinetics of [¹²⁵I]-ET-1 in CHO cells transfected with the indicated ET_A receptor mutants. All receptor mutants are compared with internalization kinetics of [¹²⁵I]-ET-1 in parallel cells transfected with wild type ET_A receptor (●). A. ET_A-T396A/S397A (○) (mutations at the P₋₁ and P₋₂ positions of the putative PDZ ligand). B. ET_A-V398A (○) and ET_A-V398G (▼) (mutations at the P₀ position of putative PDZ ligand) ET_A. C. ET_A-T403A/S404A (○) (residues of the distal β -strand). D. ET_A-I405A (○) and ET_A-I405G (▼). I405 is located in the distal β -strand region. Inlets: Agonist bound receptor (fmol/well) at plasma membrane surface at t = 0. The data are mean \pm S.D. of three parallel wells and representative of at least three independent experiments.

Fig. 7 Intracellular trafficking of ET_A receptor mutants with substitution of the putative phosphorylation sites T396, S397, T403 and S404 with alanine or negatively charged aspartic acid residues. A. Internalization kinetics of [¹²⁵I]-ET-1 in CHO cells transiently transfected with ET_A-T396D/S397D/T403D/S404D, ET_A-T396A/S397A/T403A/S404, or wild type ET_A. B Internalization kinetics of [¹²⁵I]-ET-1 in CHO cells transiently transfected with ET_A Δ 406/T396D/S397D/T403D/S404D, ET_A- Δ 406/T396A/S397A/T403A/S404A, or ET_A- Δ 406.

The data are mean \pm S.D. of three parallel wells and representative of at least three independent experiments.

Fig. 8 Lack of effect of a dominant negative EBP50 deletion mutant (EBP50 Δ ERM) on ET_A receptor internalization and recycling. Kinetics of [¹²⁵I]-ET-1 internalization in CHO cells transiently transfected with wild type ET_A receptor alone (●) or together with EBP50 Δ ERM (○). The data are mean \pm S.D. of three parallel wells and representative of at least three independent experiments. Western blot analysis of CHO cells cotransfected with HA epitope-tagged EBP50 Δ ERM confirms expression of EBP50 Δ ERM in the transfected CHO cells. A single immunoreactive band migrated at the expected molecular mass of EBP50 Δ ERM as indicated.

Fig. 9 GPCRs containing putative internal PDZ ligand motifs. Alignment of putative PDZ ligand-containing β -finger structures in the carboxyl-terminal region of GPCRs identified by an algorithm searching for conserved sequence patterns similar to that of the β -finger of nNOS. The figure shows 35 different human GPCRs identified in the analysis as described in *Materials and Methods*. Orphan receptors are indicated by asterix. The receptors are grouped according to family A, B and C GPCRs and aligned with the β -finger of nNOS. Variation in allowed β -loop length is 3-6 amino acids. Gray shading indicates conserved amino acids. All receptors contain a putative PDZ ligand with conserved amino acids at positions conforming to the P₋₂ and P₋₁ positions of class 1 PDZ ligands. In addition, all GPCRs contain a conserved positively charged residue involved in stabilization of the β -finger structure. As indicated in the figure, a few receptors contain more than one putative β -finger in the carboxyl-terminal region.

Table 1.

Radioligand binding characteristics of wild type ET_A receptor and ET_A receptor mutants

perturbing the putative recycling motif. The properties of ET-1 binding, including the number of binding sites, were determined in CHO cells transiently transfected with ET_A wild-type, ET_A-Δ406, ET_A-Δ401, ET_A-Δ390, ET_A-T396A S397A, ET_A-T403A S404A, ET_A-Δ406-GFP and ET_A-Δ401-GFP. Binding of ¹²⁵I-ET-1 was performed on membranes as described under *Materials and Methods* to determine the equilibrium dissociation constants (K_d) and the maximal binding (B_{max}) for the different receptors. The data are mean ± S.D. of three parallels and representative of at least three independent experiments.

Receptor	K_d	B_{max}
	<i>pM</i>	<i>pmol/mg</i>
ET _A wt	71 ± 3	3.2 ± 0.15
ET _A Δ406	100 ± 7	1.6 ± 0.11
ET _A Δ401	96 ± 6	1.8 ± 0.11
ET _A Δ390	87 ± 8	1.7 ± 0.55
ET _A T396A S397A	81 ± 2	3.3 ± 0.08
ET _A T403A S404A	89 ± 6	3.4 ± 0.24
ET _A Δ406-GFP	63 ± 4	6.0 ± 0.41
ET _A Δ401-GFP	139 ± 6	2.3 ± 0.10

Fig.1

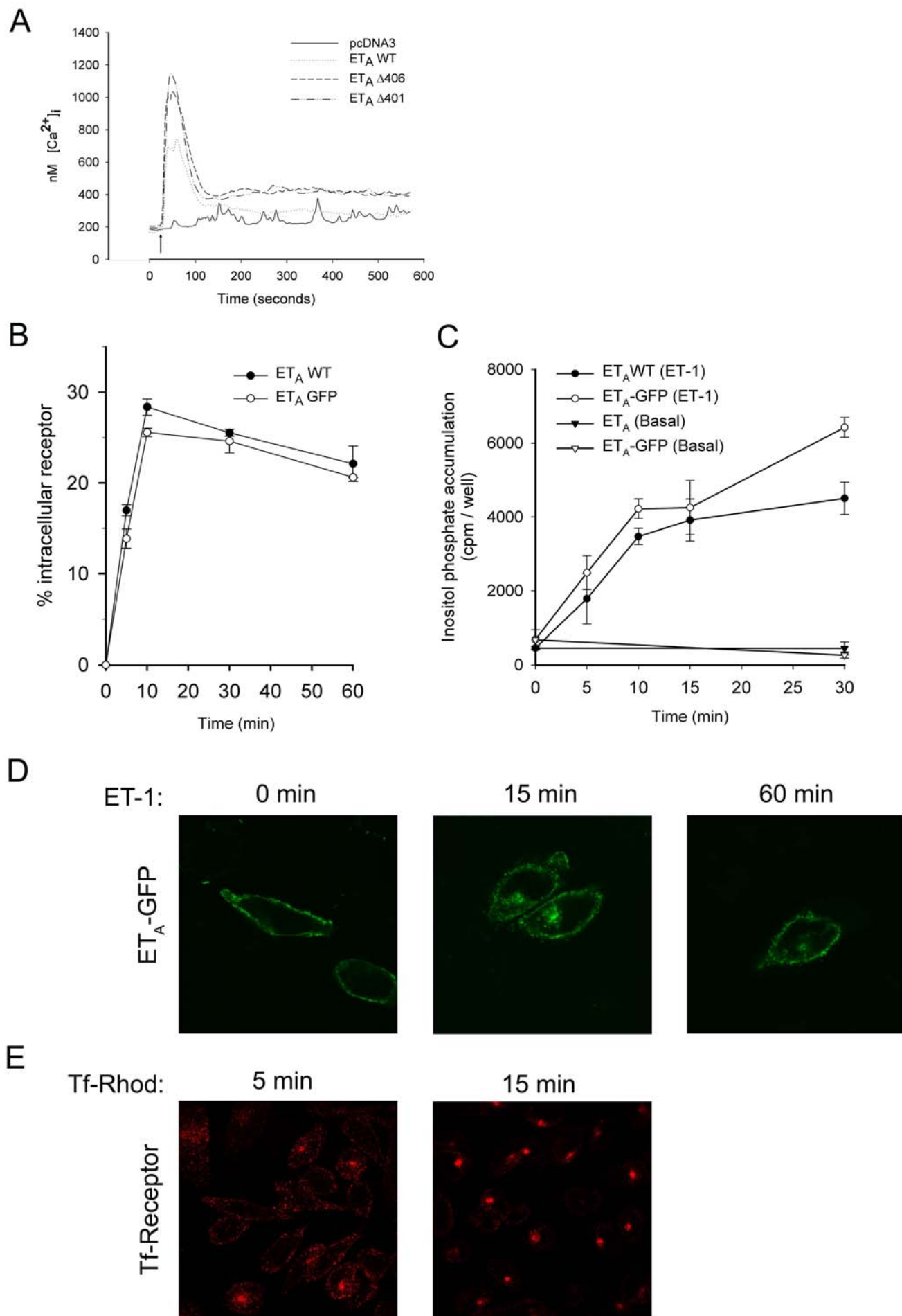


Fig.2

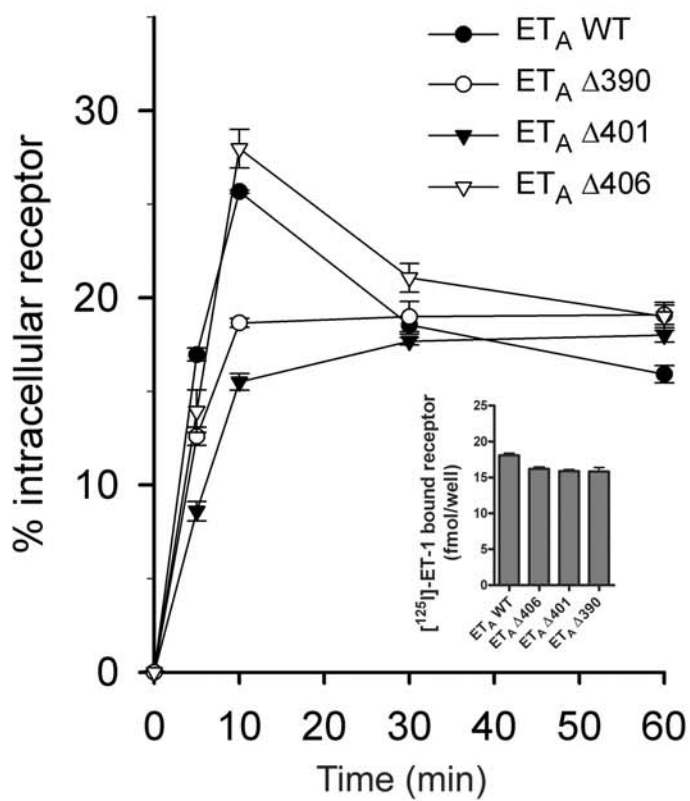


Fig. 3

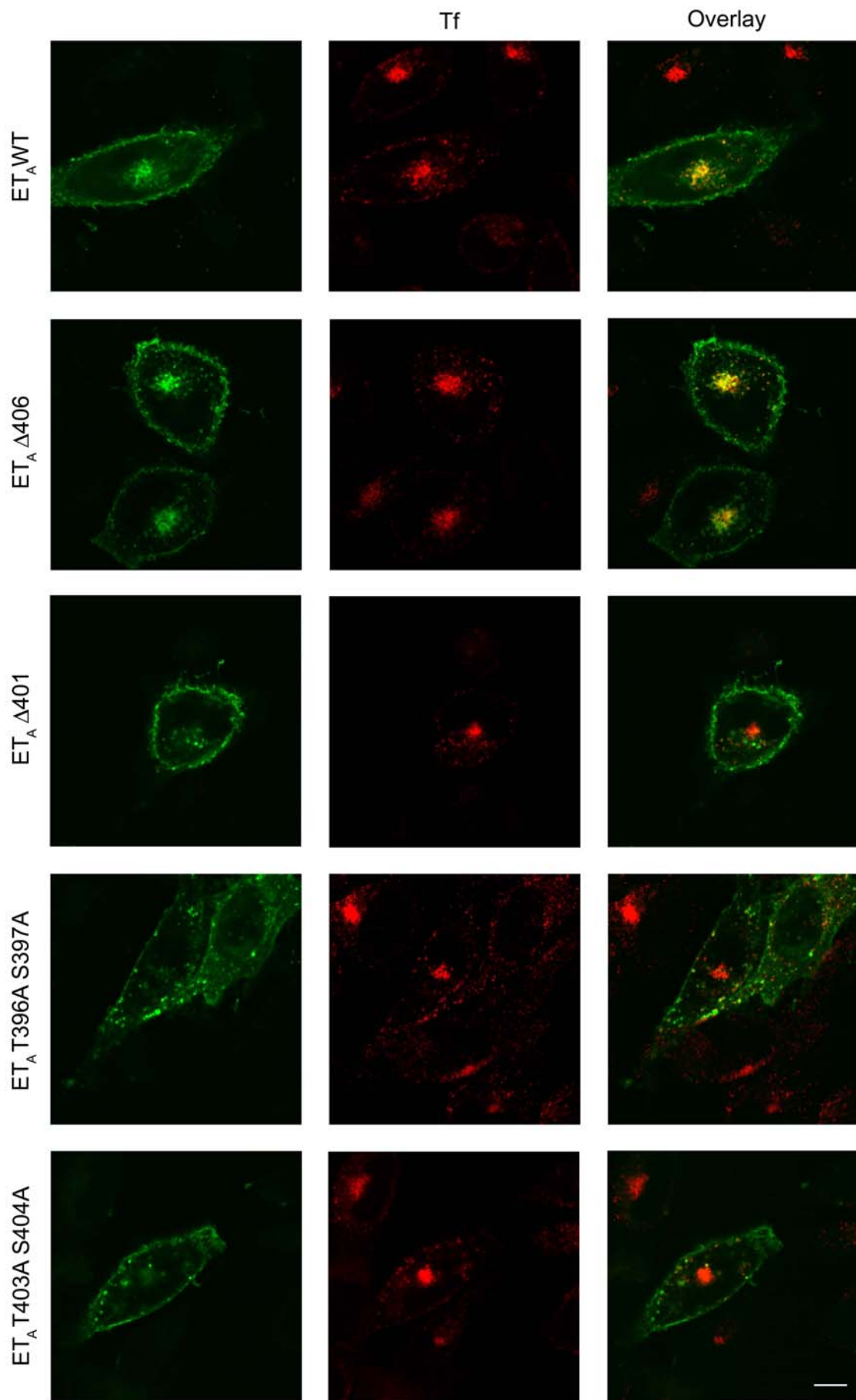


Fig. 4

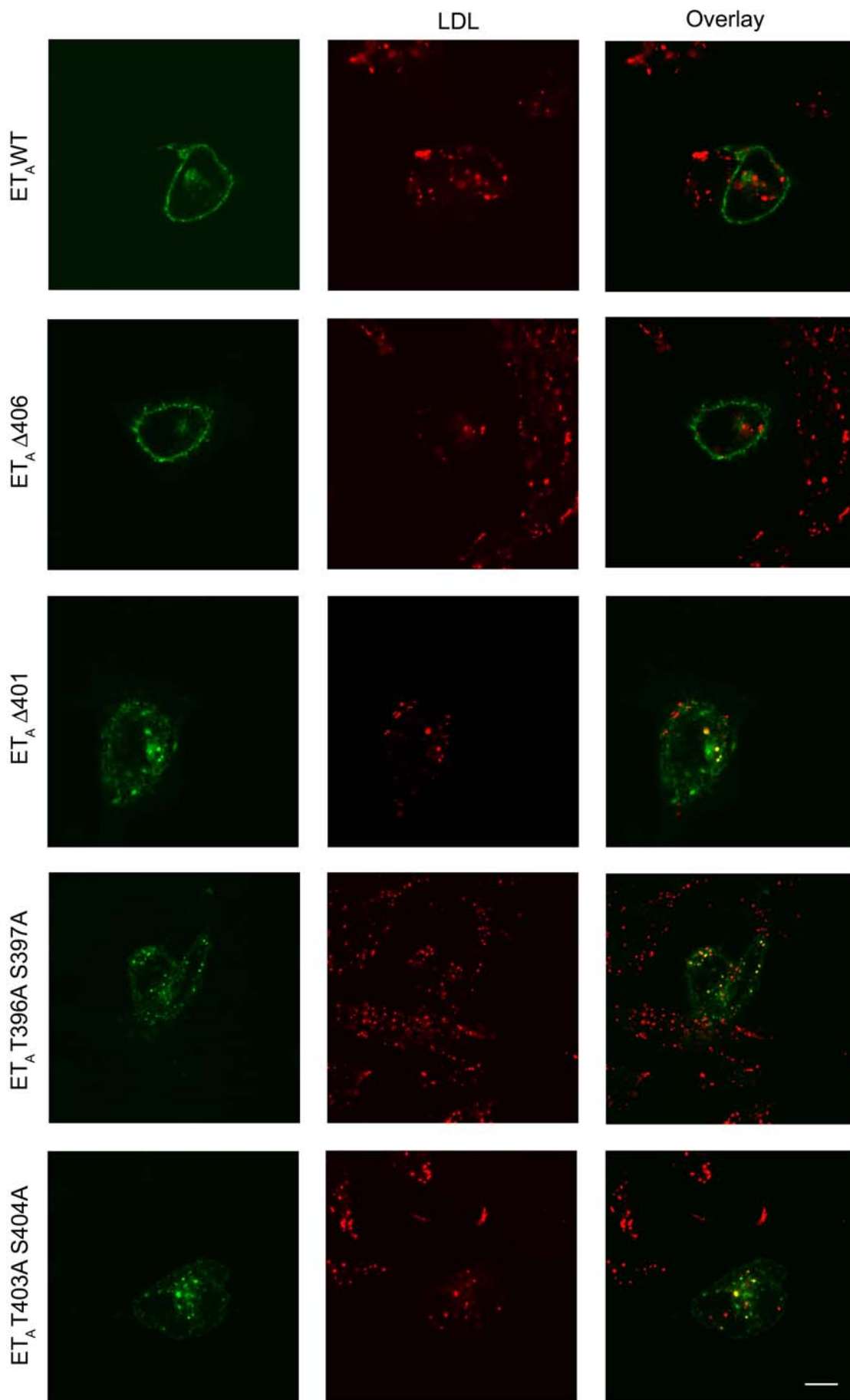


Fig.5

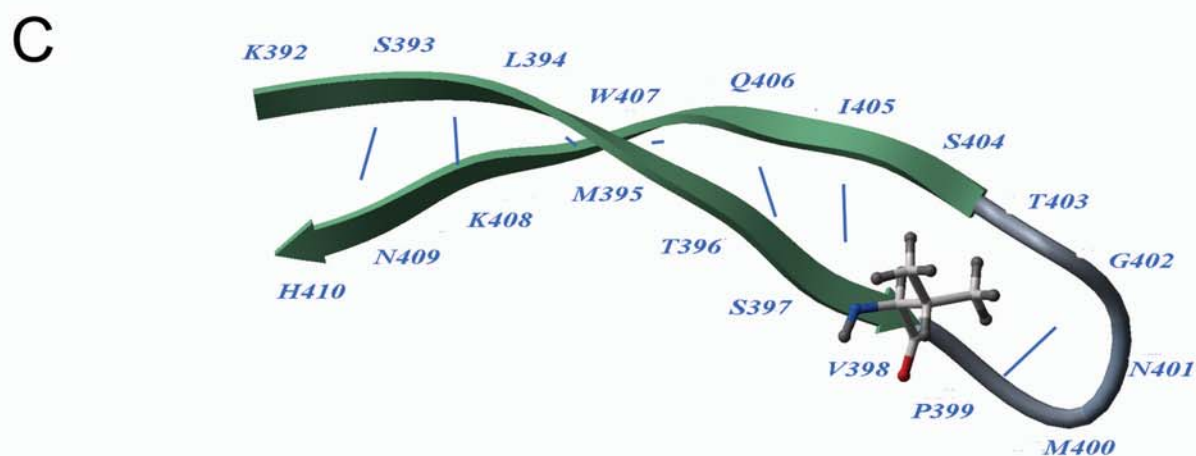
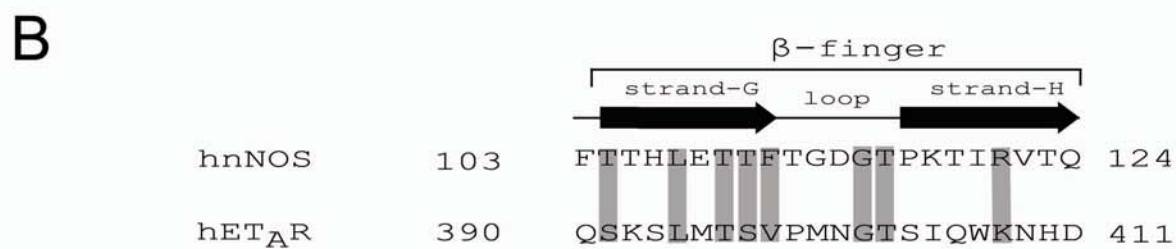


Fig.6

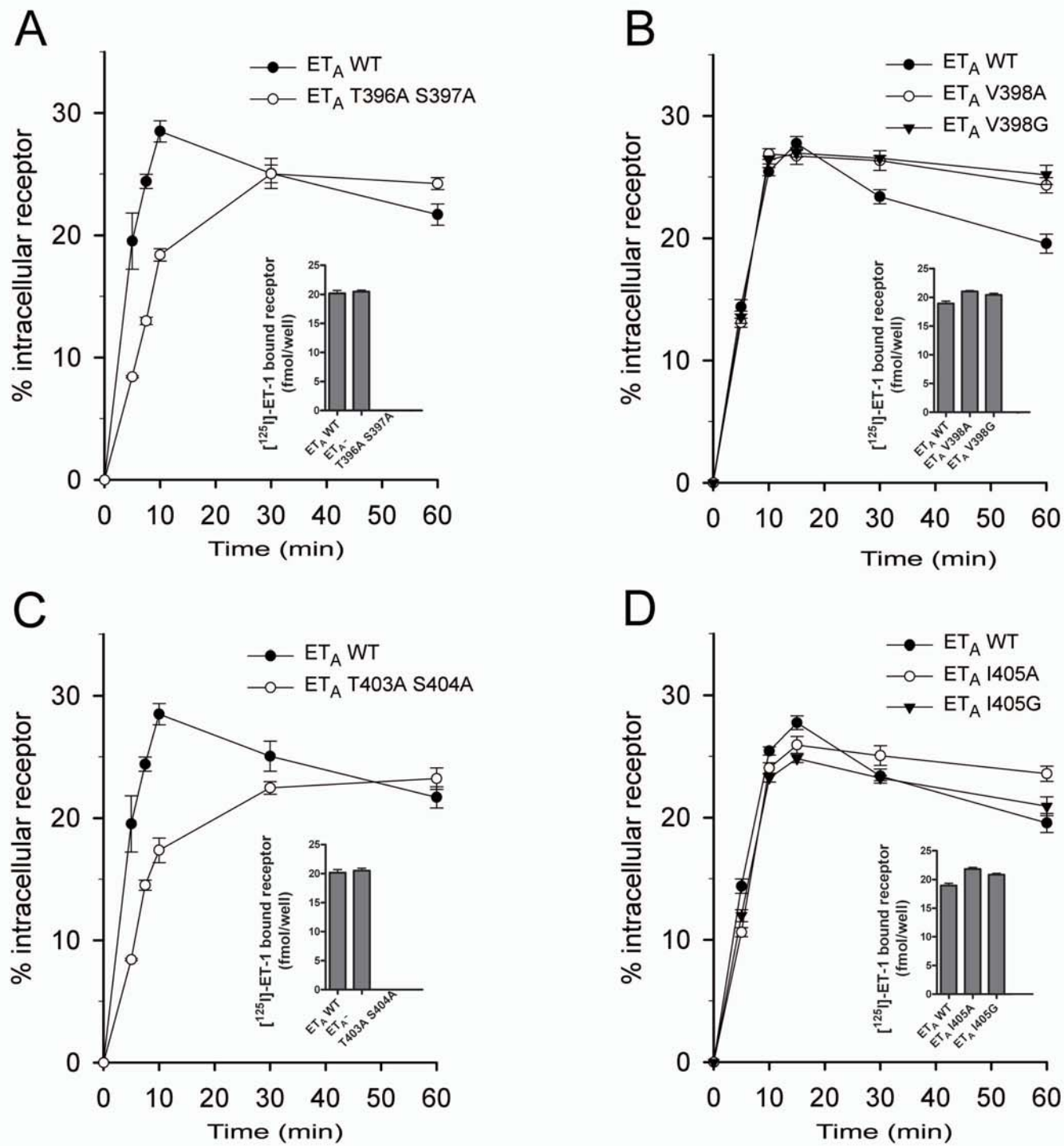
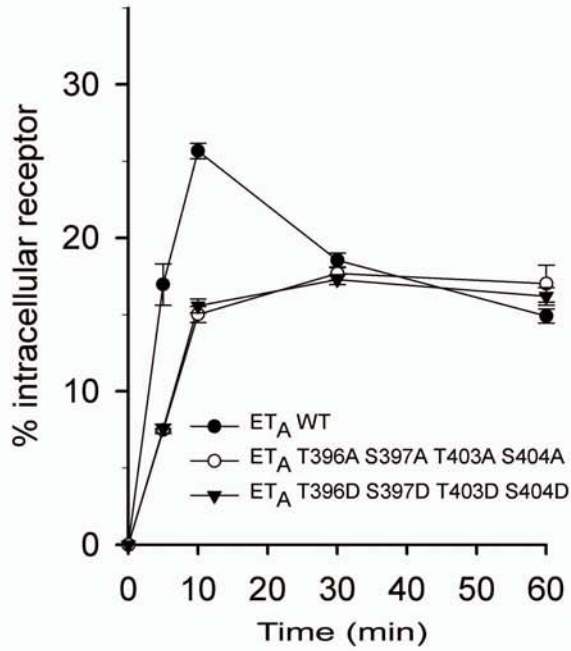
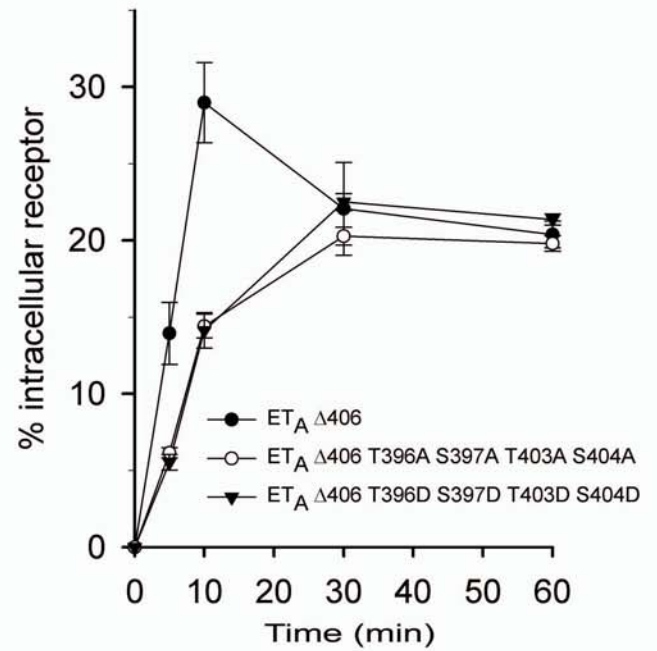


Fig.7

A



B



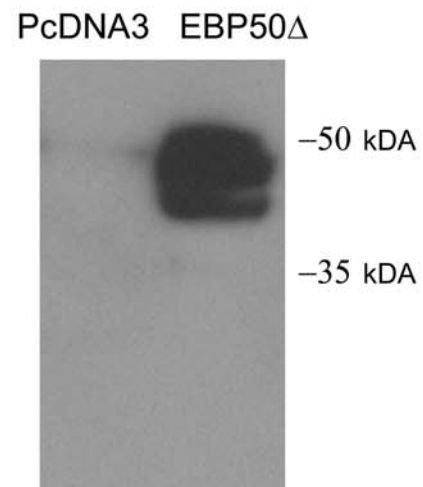
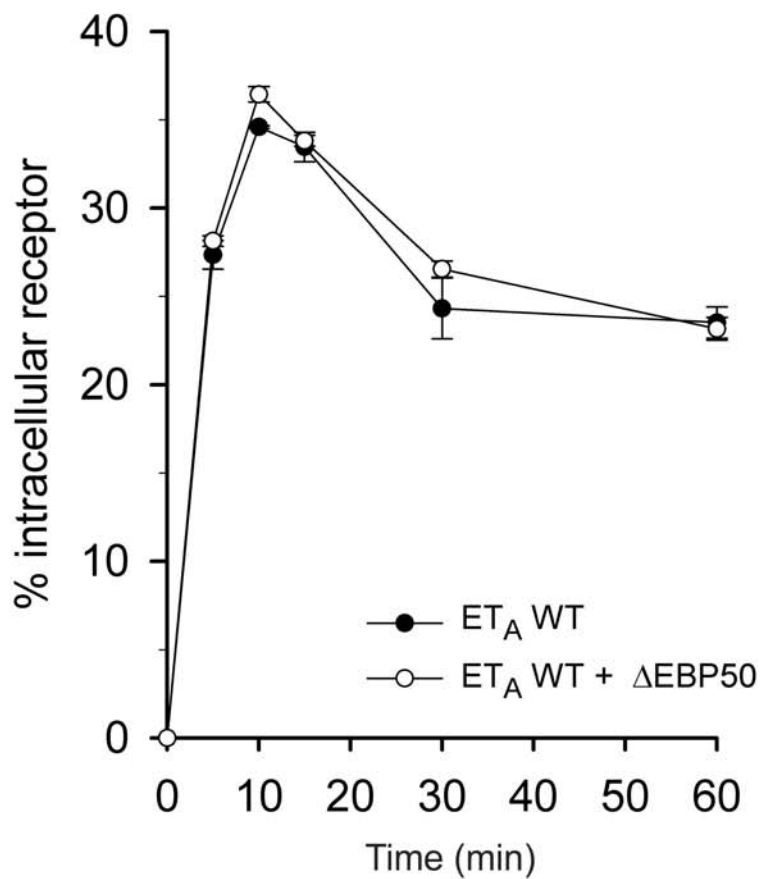


Fig.9

		β-finger				
		β-strand	loop	β-strand		
nNOS	101	EGFTTTHLETTT	--	TGDGTPKTI	RVTQ	124
A ET _A R	388	CYQ S KS L M T SV--		PMNG T SIQ W KNHD		411
AT ₁ R	320	IPPKAKSH S N L --		STKM S TLSY R PSD		343
AT ₂ R (1)	323	NRFOQ K L R SV F --		RVPI T WLQ G K R ES		346
AT ₂ R (2)	330	RSVFRVP I T W L--		QGK R ES M SCR K SSS		354
V _{1A} R	390	NNR S PTNS T G M ---		WKD S PK S SK S IK		412
BRS ₃	372	PGTGSIQ M SE I --		SVTS F TGCS V K Q AE		396
CCR ₆	336	CVRRKYK S SG F SCAG R Y S ENIS R Q T S				361
Gal ₂ R	325	AARGTHSG S V L ---		ERE S DDL L H M SE		347
NK ₁ R (1)	344	TQGS V YK V S R L--		ETT I ST V VGA H EE E		368
NK ₁ R (2)	370	EDGPKAT P S S L---		DL T SN C SS R SD S		392
NMU ₂ R	383	PCQ S SMH N SH L --		PTAL S SE Q MS R T N Y		407
Y ₁ R (1)	345	DDYETIAM S T M --		HTD V SK T SL K Q A S		368
Y ₁ R (2)	354	TMH T D V SK T SL---		KQ A SP V AF K K I N		376
Y ₄ R	347	EESEHL P L S T V --		HTE V SK G SL R LS G		370
NPFF ₁ R	373	FVVVRPSD S GL P SE S GP S GAP R PG R				398
NPFF ₂ R	477	TSNQLVQ E ST F Q N PH G ET L LY R KS A E				502
SST ₃ R	367	GKEMNGR V S Q I--		TQP G T S G Q ER P PS		390
LHR	672	PSQ S T L KL S T L --		HCQ G T A LLD K TR Y		696
α _{1D} AR (1)	500	LGPFR R PT T Q L --		RAK V SS L SH K IR A		523
α _{1D} AR (2)	529	AEAACAQ R SE V ---		EAV S L G VP H EV A		551
β ₃ AR	374	AARPAL F PS G V--		PAAR S SPA Q PR L C Q		398
5HT _{2A} R	436	AKT T D N DC S M V AL G K Q H S E E AS K D N S				461
DP ₂ R	323	LESVLVDD S E L --		GGAG S SR R RR T SS		346
LPA ₄ R	324	INAHIR M ES L F---		KT E T P L T T K PS L		346
S1P ₄ R	345	HSGAST T D S SL--		RPRD S FR G S R S L S		368
GPR75*	446	CGP S HS K ES M V--		SP K IS A GH Q H C G Q		469
H963*	286	YH L SK A FR S K V --		T E T F AS P K E T K A Q K		310
HM74*	348	NSG E P W SP S YL---		G P T S NN H S K KG H		370
CMKLR1* (1)	324	KKFK V AL F S R L--		V N AL S ED T G H SS Y		347
CMKLR1* (2)	346	SYP S HR S F T K M SS M N E R T S M N E R E T G				371
CMKLR1* (3)	349	SHR S F T K M SS M ---		NER T S M N E R E T G		371
GPR25*	328	LARRISS A SS L --		SRDD S SV F RC R A Q A		352
SALPR* (1)	394	REFRK A L K S L L W RIAS P S I T S M R P F T				419
SALPR* (2)	405	WRIAS P S I T S M--		RP F T A T T K P E H E D Q		427
LGR ₅ *	802	VWTRSK H PS L M---		S I NS D D V E K Q S C		824
B PAC ₁ R	436	ASSGVNG G T Q L--		SIL S K S SS Q IR M S G		460
VPAC ₁ R (1)	424	GSNGAT C ST Q V S ML T RV S PGARR S SS				449
VPAC ₁ R (2)	427	GATC S T Q V S ML---		TR V SP G ARR S SS		449
PTH ₂ R	461	SQS Q VAA S T R M---		V L IS G KA A K I AS		483
C mGlu ₅ R	1048	ARS S SS Q G S LM---		EQ I SS V VT R FT A		1070
GABA _{B1} R	902	IAEKEER V SE L --		RH Q L Q SR Q LR S RR		926
GABA _{B2} R	905	PSIG G VD A SC V SP C VS P T A SP R H R H V				930
GABA _{BL} R* (1)	602	RRAAQ R AR S H F --		PG S AP S SV G H R AN R		626
GABA _{BL} R* (2)	610	SH F PG S AP S SV G H R AN R T V PG A H S R L				635